

PAPER • OPEN ACCESS

Adsorption of Cu(II) Ions in Aqueous Solutions by HCl Activated Carbon of Oil Palm

To cite this article: A Muslim *et al* 2017 *IOP Conf. Ser.: Mater. Sci. Eng.* **206** 012075

View the [article online](#) for updates and enhancements.

You may also like

- [The physical properties observation of oil palm empty fruit bunch \(OPEFB\) chemical treated fibres](#)
M K Faizi, A B Shahrman, M S Abdul Majid *et al.*
- [Anaerobic digestion of fungally pre-treated oil palm empty fruit bunches: energy and carbon emission footprint](#)
N Hidayat, S Suhartini, R N Utami *et al.*
- [Oil Palm Empty Fruit Bunch \(OPEFB\) Pellets as a Biosorbent for Ni \(II\) and Cr \(VI\) removal in an aqueous solution](#)
N F Muhamad Salleh, N A Ghafar, N Mohd Shukri *et al.*



ECS
The
Electrochemical
Society
Advancing solid state &
electrochemical science & technology

DISCOVER
how sustainability
intersects with
electrochemistry & solid
state science research

Adsorption of Cu(II) Ions in Aqueous Solutions by HCl Activated Carbon of Oil Palm

A Muslim*, Y Syamsuddin, A Salamun, Abubakar, D Ramadhan, D Peiono

Process Technology Laboratory, Department of Chemical Engineering Faculty of Engineering, Syiah Kuala University, Banda Aceh 23111, Indonesia

E-mail: abrar.muslim@che.unsyiah.ac.id

Abstract. Activated carbon was prepared from oil palm empty fruit bunch (OPEFB) by pyrolysis at 873.15 K in a furnace and chemical activation using 0.01 M HCl. Fourier Transform Infrared Spectroscopy, Scanning Electron Microscopy and BET (Brunauer, Emmett and Teller) surface area analyses were taken into account to investigate the chemical functional group, to characterise the surface morphology and to determine total surface area the OPEFB AC, respectively. Experiments in batch mode were conducted to investigate Cu(II) adsorption capacity by the OPEFB AC whereas the system consisted of 1 g the OPEFB AC in 100 mL Cu(II) aqueous solution with initial concentration in the range of 10-70 mg/L, magnetic stirring at 75 rpm, room temperature of 300.15 K (± 2 K), at 1 atm and neutral pH over contact time in the range of 0-150 min. As the result, Cu(II) adsorption capacity increased exponentially over contact time and initial concentration. The Cu(II) adsorption kinetics followed the pseudo second order kinetics with the correlation coefficients (R^2), kinetics rate constant and equilibrium adsorption capacity being 0.98, 4.81 mg/g and 0.15/min, respectively for initial Cu(II) concentration being 58.71 mg/L. In addition, Cu(II) adsorption isotherm followed the Langmuir equation with the R^2 value, the mono-layer and over-all adsorption capacity being 0.99, 5.92 mg/g and 0.17 L/mg, respectively.

1. Introduction

Heavy metals are hazardous and non-biodegradable pollutants in the environment and can be accumulated in the human body. Waste water consisting of heavy metals can be released to the environment from industrial processes such as paper and rubber, mining, petroleum refining, electroplating and smelting [1], [2], [3], [4], [5]. Cu(II) ion is one of the most hazardous ions of heavy metals contained in the wastewater from mining, chemical and electrical industries [6]. It can bio-accumulate in the human body tissues leading to organ cancer and disorder of biological system of human body [7]. Therefore, removing copper from Cu(II) ions-contaminated wastewater is needed before releasing to the environment.

Membrane filtration, electrolysis, chemical precipitation and adsorption using activated carbon have proposed to remove heavy metal ions from inorganic wastewater, and adsorption is one of effective and promoting processes to apply [8], [9]. Wastes from agricultural industries have been investigated to prepare as alternative raw material of adsorbents because it is more economically and environmentally applied compared to others. Utilisation of adsorbents from agricultural wastes which were coarse tea, green tea, Brazil nut shells, coffee bean husks and areca catechu shell, had been investigated for the adsorption of Cu(II) ions from aqueous solutions [10], [11], [12], [13].



Interestingly, oil palm empty fruit bunch (OPEFB) has been proposed as raw material of activated carbon using KOH activator for adsorption of malachite green [14].

The OPEFB as one of waste types from palm oil production is becoming an attractive renewable material for activated carbon because the world palm oil production was projected to sustained and impressive growth in the period of 2016–2020 [15] with the average annual world production of palm oil predicted to be more than 30 million tonnes consisting of approximately 15 million tonnes from Malaysia and the same amount from Indonesia. Indonesia was projected becoming the world's largest exporter and producer of palm oil taking over Malaysia [16]. Hence, it is necessary to investigate the utilisation of carbon active from the OPEFB for adsorption of heavy metal including Cu(II) to answer the global consumption of activated carbon which has been increasing and was forecasted to reach approximately 1.733 million tons by the next two years [17].

This study aimed to prepare activated carbon from the OPEFB for adsorption of Cu(II) ions from aqueous solutions. The chemical functional groups and surface morphology of the OPEFB, carbon and activated carbon were analysed using Fourier transform infrared spectroscopy (FTIR) and scanning electron microscopy (SEM), respectively. This preliminary study was performing by conducting experiments in batch mode at room temperature and neutral pH to obtain Cu(II) adsorption isotherms and kinetics parameters.

2. Materials and method

2.1. Activated carbon from the OPEFB

Preparation of the OPEFB activated carbon (OPEFB AC) and the adsorption experiments in batch mode were done in the Process Technology Laboratory at Department of Chemical Engineering, Syiah Kuala University. An atomic absorption spectrometer (AAS) (Shimadzu AA 6300, made in Japan) in Chemical Analysis Laboratory at the Faculty of Mathematics and Science, Syiah Kuala University was used to obtain Cu(II) ions concentration in the aqueous solution. Nova Station C (Quantachrome Instruments version 11.0, made in USA) which was available in Instrument Laboratory (ITB, Bandung) was used to obtain the BET surface area, pore size and total pore volume of the OPEFB AC.

The OPEFB waste were collected from palm oil processing plant of PT. Mopoli Raya, West Aceh. The OPEFB of 1 kg was washed wholly using tap water and distilled water at the end. It was dried under the sun for 7 days at average temperature of 304.15 K (± 2 K) and relative humidity of 12.5%. The dried OPEFB were crushed to powder using a ball mill. Pyrolysis of the OPEFB was performed using the same method presented in previous study [18] by coating the dried OPEFB with at least four layers of aluminum foil in a Nabertherm furnace (More Than Heat 30-3000 °C, made in Germany) at 873.15 K for 1 h. Then, the OPEFB carbon of 500 g was activated using 0.01 M HCl (Gatt-Koller) in 1000-mL beaker without stirring it for 2 h. The OPEFB activated carbon was washed and decanted many time with distilled water until reaching pH 7 (± 0.5 K) to remove the excess acid, and it was then filtered using vacuum filter. To remove the excess water, the OPEFB activated carbon was dried in a Memmert oven (NN-ST342M, made in Germany) at 373.15 K until reaching a constant weight. It was sieved to obtain a uniform size of 100 mesh. The OPEFB activated carbon was stored in sealed plastic bottle to use within 2 weeks for experiments.

2.2. Characterization of the OPEFB

Chemical functional groups on the OPEFB powder and activated carbon were identified using the FTIR. The FTIR spectra were obtained between 400 and 4000 cm^{-1} of wavenumber using a Spectrophotometer (Shimadzu IR Prestige 21, made in Japan) which is available in the Analysis Instrument Laboratory of Chemical Engineering Department of Syiah Kuala University, and KBr pellets of 0.1% sample were used to obtain the transmission spectra of the samples. Meanwhile, the physical morphology of the OPEFB powder, carbon and activated carbon surface were identified using a HITACHI TM3000 scanning electron microscopy (made in Japan) with an accelerating voltage of 500VA (1 phase of 50/60Hz) which is available at Mechanical Engineering Department of Syiah Kuala University. All the samples were dried in an oven at 293.15 K for about 10 min prior to

the SEM analysis. Prior to measurement of the BET surface area, pore size and total pore volume of the OPEFB, the OPEFB AC sample of 0.039 was degassed under relative pressure in range of 0-1 at 573.15 K for 3 h.

2.3. *Cu(II) aqueous solution*

The Cu(II) aqueous solution of 1000 mg/L was prepared by dissolving 3.97 g (± 0.001) $\text{CuSO}_4 \cdot 5\text{H}_2\text{O}$ (99% pure from Aldrich) in 1000 mL distilled water in 1000-mL Erlenmeyer flask. The sample of 5 mL was taken from stock solution and analyzed using Atomic Absorption Spectrophotometer (AAS) to obtain the Cu(II) concentration. To prepare all the predetermined concentration of aqueous solution for adsorption experiments, the stock solution was taken using a variable volume pipette, and it was diluted with distilled water to obtain the predetermined Cu(II) concentration calculated based on general dilution formula.

2.4. *Adsorption kinetics and isotherm experiments*

To obtain an equilibrium time for the Cu(II) ions adsorption on the OPEFB activated carbon, a Cu(II) adsorption experiment of was conducted in batch mode based on the procedure proposed in the literature [14]. The OPEFB activated carbon of 1 g was placed into a 200-mL erlenmeyer flask, and it was mixed with 100 mL of Cu(II) aqueous solution. The set initial concentration was 50 mg/L but based on the AAS reading, it was 49.99 mg/L. The mixture set at neutral pH was stirred using a magnetic stirrer at 75 rpm, room temperature of 300.15 K (± 2 K) and 1 atm. The sample of 1 mL was taken using a variable volume pipette at the predetermined contact time of 0, 15, 30, 45, 60, 75, 90, 105 and 120 min and stirring was stopped for 1 min before sampling. Each sample was added to 5 mL of distilled water in a separated 10-mL vial for the AAS analysis. To determine the real concentration of samples, the dilution factor was taken into account to the concentration calculated from the AAS reading. Based on this experiment, the Cu(II) adsorption reached equilibrium contact time at 120 min. The experiment was repeated for lower Cu(II) initial concentration of 60 mg/L (58.71 mg/L based on the AAS reading) to investigate the effect of initial Cu(II) concentration on adsorption kinetics parameters.

Experiments of adsorption isotherm were conducted at neutral pH, 75 rpm stirring, room temperature of 300.15 K (± 2 K) and 1 atm. The experiment procedure of adsorption kinetics mentioned above was used for adsorption isotherm experiments with the predetermined Cu(II) initial concentration varied in the range of 10-70 mg/L. The samples of 1 mL for the AAS analysis were taken at the contact time of 0 and 120 min.

3. Results and discussion

3.1. *Chemical functional groups*

The chemical functional groups of the OPEFB powder and the OPEFB AC was obtained using the FTIR spectra in 400-4000 cm^{-1} range, as can be observed in figure 1. As can be seen in figure 1, there would be seven major absorption bands obtained from the spectra of the OPEFB powder and the OPEFB AC. The first band would be at approximately 3500-3700 cm^{-1} of wavenumber with a peak at approximately 3614.61 cm^{-1} , indicating the O-H stretching group of phenol and alcohol [19]. The second band is the C-H stretching with a wide band at approximately 2700-2980 cm^{-1} and 2 intense bands at approximately 2926.01 and 2858.51 cm^{-1} , presenting aldehyde. The third band is in 1500-1700 cm^{-1} range with the peaks at approximately 1687.71 and 1550.77 cm^{-1} that is assigned the C=C stretching of alkene [20]. The fourth band is the C-H symmetrical and asymmetrical bending with the band at approximately 1317-1450 cm^{-1} [21] and the peak at approximately 1456.26 cm^{-1} . Other bands are for the C-O stretching of aromatic ether and ester in 1240-1284 cm^{-1} range with the peak at approximately 1269.16 cm^{-1} , and for the C-O stretching of carboxylic acids esters in 1000-1260 cm^{-1} range [21] with the peak at approximately 1120.64 cm^{-1} . The last band is a weak band which is associated to the C-C stretching at 400-800 cm^{-1} with the intense bands at approximately 758.02 and 563.21 cm^{-1} .

As shown by the FTIR spectra in figure 1, it can be noticed that pyrolysis at 873.15 K for 1 h followed 0.01 M HCl chemical activation decreased the O–H stretching in the OPEFB powder as indicated by the incline in the transmittance of from 85.24 to 80.78%. It means that phenol and alcohol were removed by approximately 5.23% during the utilisation of the OPEFB AC from the OPEFB powder. The utilisation can break the C–H stretching in the OPEFB which is shown by the decrease in the transmittance of the first and second peak from approximately 83.14 to 76.49% and from approximately 84.42 to 78.7%, respectively. As the result, aldehyde in the OPEFB was removed by approximately 14.77%. A higher amount of decrease in chemical functional groups was occurred in the OPEFB powder whereas the C=C stretching transmittance dropped from approximately from 78.91 to 70.73% and from 77.61 to 70.07% for the first and second intense bands, respectively. It indicated that alkene from the C=C stretching was released by approximately 20.08% during the preparation of the OPEFB AC from the OPEFB powder. In addition, alkene from the C–H symmetrical and asymmetrical bending was also released, and it was approximately 11.12% fall shown by the fall in the peak transmittance being falling from 79.02 to 70.23%, as can be seen in figure 1.

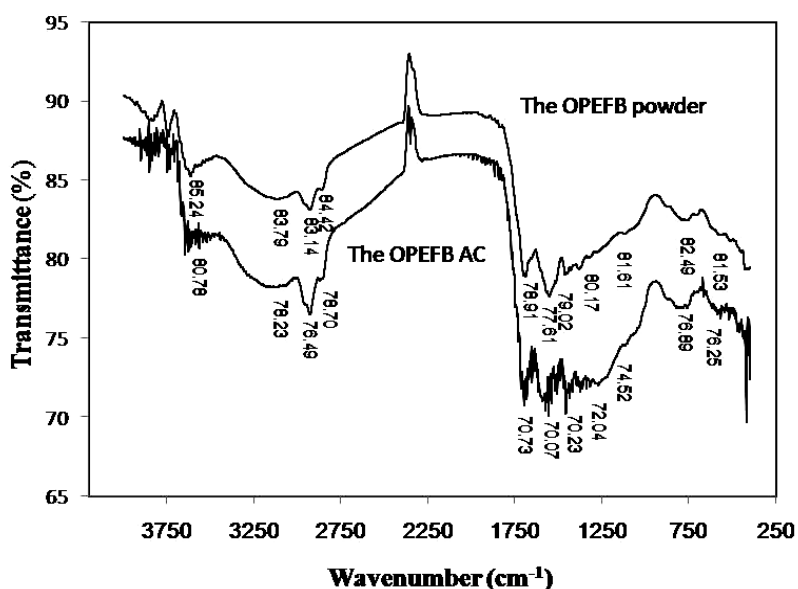


Figure 1. The FTIR spectra of the OPEFB powder and OPEFB AC.

3.2. Surface morphology of the OPEFB activated Carbon

Figures 2(a) and (b) show the SEM micrographs (2000X) of the surface morphology of the OPEFB powder and the OPEFB AC, respectively. A considerable amount of ether and ester in the C–O stretching was removed from the OPEFB powder during the utilisation of the OPEFB AC, and it was by 18.83% indicated by the decrease in the peak transmittance of the C–O stretching of aromatic ether and ester from 80.17 to 72.04% and the decrease in the peak transmittance of the C–O stretching of carboxylic acids esters from 81.61 to 74.52%. Moreover, the last band peak associated to the C–C stretching also reduced by 15.47% from 84.49 to 76.89% for the first peak and from 81.53 to 76.25% for the second peak. Overall, the utilisation of the OPEFB AC from the OPEFB powder reduces the chemical functional groups such as phenol, alcohol, aldehyde, alkene, ether, ester and internal carbon stretching leading to the formation of pores and active site on the OPEFB AC. However, from the transmittance value of 74.64% on average, there could be less pores and active site formed on the OPEFB AC for the adsorption of Cu(II) ions.

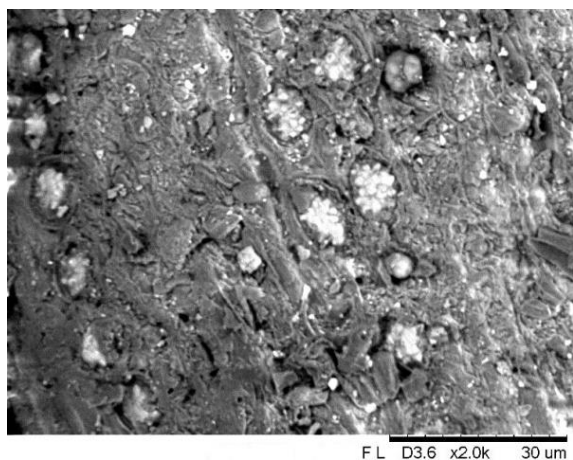


Figure 2(a). The SEM micrographs of the OPEFB

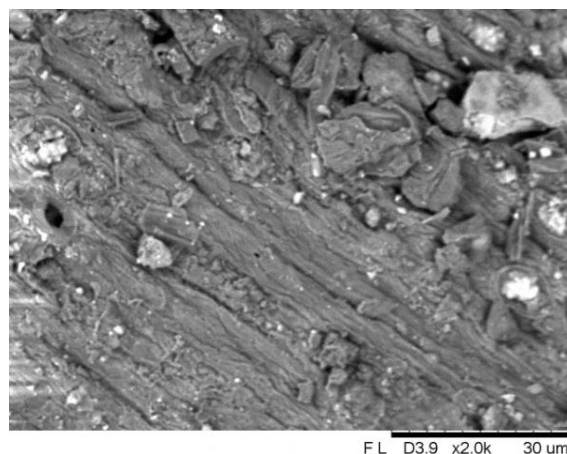


Figure 2(b). The SEM micrographs of the OPEFB AC

As shown in figure 2(a), there are almost regular pores on the OPEFB powder surface, and round materials like flower are in the pores. It seems that the round materials indicate the chemical functional groups of the OPEFB powder, as also highlighted in the previous study [13]. Meanwhile, the round materials of volatile species are not absent at all on the OPEFB AC, as can be seen in figure 2(b). Low concentration of HCl (0.01 M) could be the reason for this. Interesting to note that the pores size and the amount of pores on the OPEFB AC is still small. It could be because the HCl activator concentration being used was still small (0.01 M) to break the C–C stretching and to remove all the volatile matters in the OPEFB powder, as also shown by the overall transmittance in figure 1. Less pores of the OPEFB AC may be formed leading to less surface area, pore size and total pore volume of the OPEFB AC. This expectation was also in line with the results of BET analysis whereas the total surface area, pore volume and pore diameter of the OPEFB AC was 438 m²/g, and 9.431e-03 cc/g, respectively with the pore diameter being 2.638e+02 Å.

3.3. Effect of contact time on Cu(II) adsorption capacity

A batch mode experiment of Cu(II) adsorption was conducted to investigate the effect of contact time on Cu(II) adsorption capacity by the OPEFB AC. The experimental condition shown by the figure 3 legend whereas the system consisted of 50 mg/L Cu(II) initial concentration and 1 g the OPEFB AC.

As the result, Cu(II) adsorption capacity by the OPEFB AC sharply increased during 30-min contact time from 0 to 3.66 mg/g. It moderately inclined to 4.08, 4.25, 4.41 and 4.58 mg/g at 60, 90, 120 and 140-min contact time, respectively. It is clear to see in figure 3 that it reached equilibrium contact time of 140-min because it did not change to much when the contact time increased to 150-min, which was 4.59 mg/g. Overall, Cu(II) adsorption capacity by the OPEFB increased exponentially over contact time until reaching a maximum adsorption capacity, and the same trends also presented in the previous studies [13], [21], [22], [23].

3.4. Effect of contact time on Cu(II) adsorption capacity

The experiments with predetermined initial concentration of Cu(II) ions varied from 10 to 70 mg/L were performed to investigate the effect of initial Cu(II) concentration on the adsorption capacity by the OPEFB AC. As the result, Cu(II) the adsorption capacity by the OPEFB AC considerably increased from 0.87 to 2.26, 3.26, 4.59 and 4.83 mg/g for the increase in the initial Cu(II) concentration in solution from 10 to 30, 40, 50 and 60, respectively, as can be observed in figure 4. However, it fell a bit to 4.62 mg/g when the the initial Cu(II) concentration decreased to 70 mg/g. Overall, Cu(II) adsorption capacity by the OPEFB AC increased exponentially for the increasing

initial Cu(II) concentration in solution from 10 to 70 mg/L even if it was a bit fall at 70 mg/L. The same trend also reported in the previous studies [13], [24].

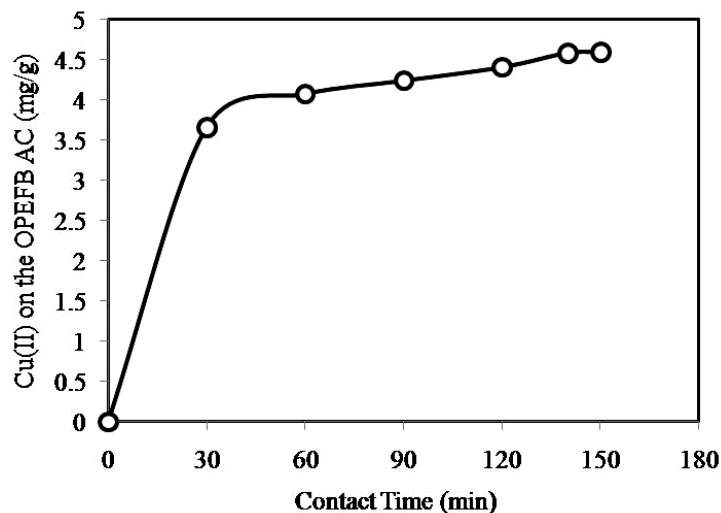


Figure 3. Contact time versus Cu(II) adsorption capacity of the OPEFB AC. Experimental condition: 100 mL aqueous solution of 50 mg/L initial Cu(II) concentration, 1 g the OPEFB AC, 75 rpm magnetic stirring, room temperature of 300.15 K (± 2 K), neutral pH and 1 atm.

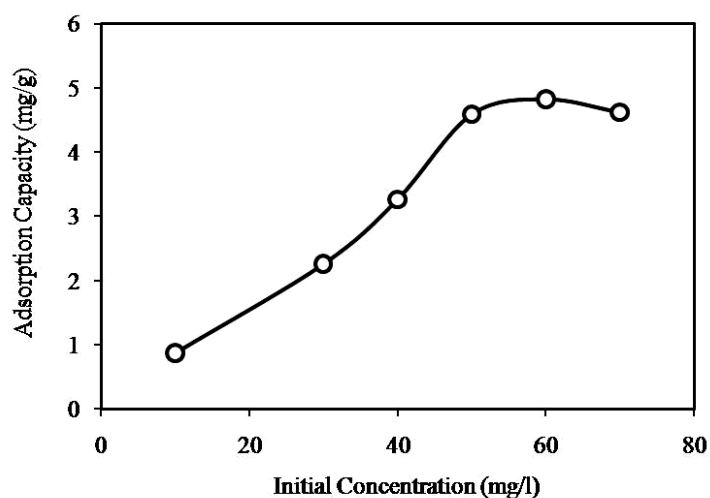


Figure 4. Effect of initial Cu(II) concentration in solution on the adsorption capacity by the OPEFB AC. Experimental condition: 100 mL aqueous solution of Cu(II) ions with initial concentration varied from 10 to 70 mg/L, 1 g the OPEFB AC, 75 rpm magnetic stirring, room temperature of 300.15 K (± 2 K), neutral pH and 1 atm with sampling time of 150-min.

3.5. Cu(II) adsorption kinetics by the OPEFB AC

Adsorption kinetics of Cu(II) by the OPEFB AC represents the amount of Cu(II) adsorbed by the OPEFB AC over time. It can be examined by obtaining the deviation of Cu(II) concentration in solution over contact time, and it can present the rate constant of Cu(II) adsorption on the OPEFB AC.

The common equations are presented by equations (1) and (2) for the pseudo first order [25] and the pseudo second order models [26], respectively:

$$\frac{dq_t}{dt} = k_L (q_e - q_t) \quad (1)$$

$$\frac{dq_t}{dt} = k_H (q_e - q_t)^2 \quad (2)$$

where q_t (mg/g) is the Cu(II) adsorption capacity by the OPEFB AC at the time of t (min), q_e (mg/g) denotes the equilibrium adsorption capacity, k_L represents the rate constant of pseudo first order model (min^{-1}), and k_H is the rate constant pseudo second order model (g/mg.min). Linearizing equations (1) and (2) by integration of equations (1) and (2) with the boundary conditions $q_t = 0$ mg/g ($t = 0$ s) and $q_t = q$ mg/g ($t = t$ s), results in equations (3) and (4), respectively [13]:

$$\log(q_e - q_t) = \log q_e - \left(\frac{k_L t}{2.303} \right) \quad (3)$$

$$\frac{t}{q_t} = \frac{1}{k_H q_e^2} + \frac{t}{q_e} \quad (4)$$

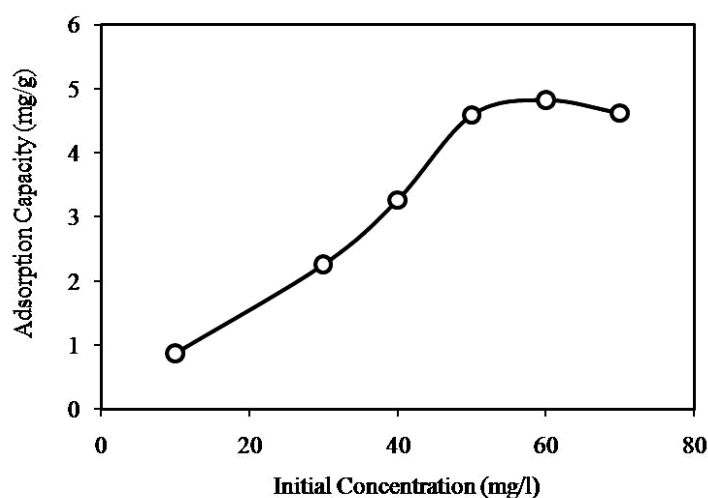


Figure 5. Pseudo first order kinetics of Cu(II) adsorption on the OPEFB AC. Experimental condition: 100 mL aqueous solution of Cu(II) ions with initial concentration varied being 49.99 and 50 mg/L, 1 g the OPEFB AC, 75 rpm magnetic stirring, room temperature of 300.15 K (± 2 K), neutral pH, 1 atm and contact time of 0, 30, 60, 90, 120, 140 and 150 min.

The pseudo first order and second order models were plotted using the data shown in figure 5 and the data from the second experiment of Cu(II) adsorption kinetics with Cu(II) initial concentration being 58.71 mg/L. The Cu(II) adsorption capacity obtained at the contact time of 0, 30, 60, 90, 120, 140 and 150 min was 0, 2.89, 4.09, 4.29, 4.39, 4.47 and 4.65 mg/L, respectively.

The results of Cu(II) adsorption kinetics are shown in figures 5 and 6. As clearly shown by the legends in figures 5 and 6, the Cu(II) adsorption kinetics on the OPEFB activated carbon follows the pseudo second order kinetics, which was justified by the correlation coefficients, R^2 for the pseudo second order kinetics (0.99 and 0.98) being much higher than the pseudo first order kinetics (0.292 and 0.350).

The rate constants of pseudo second order kinetics, k_L and the equilibrium adsorption capacity, q_e determined was 0.19 /min and 4.69 mg/g, respectively for 49.99 mg/L initial Cu(II) concentration, and it was 0.15 /min and 4.81 mg/g, respectively for 58.71 mg/L initial Cu(II) concentration. It means that increasing initial Cu(II) concentration in solution from 49.99 to 58.71 mg/L lifted up the equilibrium adsorption capacity by 2.4%. The increase in the equilibrium adsorption capacity is reasonable because all the active sites on the OPEFB AC could not be completely occupied Cu(II) ions at 50 m/L initial Cu(II) concentration due to the amount of Cu(II) ions could be still less than the available active sites on the OPEFB AC. Meanwhile, the increase in the adsorption kinetics rate constant was caused by the higher driving force to transport Cu(II) ions in solution onto the OPEFB AC overtime, whereas it was caused by the higher deviation between mass of Cu(II) ions in solution and on the OPEFB AC when the higher initial Cu(II) concentration was applied. In other words, the higher initial Cu(II) concentration, the faster adsorption of Cu(II) ions onto the OPEFB AC occurred.

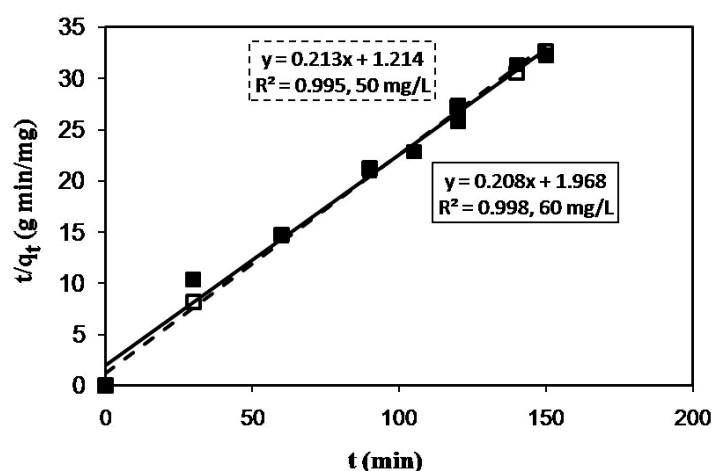


Figure 6. Pseudo second order kinetics of Cu(II) adsorption on the OPEFB AC. Experimental condition: 100 mL aqueous solution of Cu(II) ions with initial concentration varied being 49.99 and 50 mg/L, 1 g the OPEFB AC, 75 rpm magnetic stirring, room temperature of 300.15 K (± 2 K), neutral pH, 1 atm and contact time of 0, 30, 60, 90, 120, 140 and 150 min.

3.6. Cu(II) adsorption isotherm by the OPEFB AC

The adsorption isotherm equations of Langmuir and Freundlich were used to determine the Cu(II) adsorption isotherm by the OPEFB AC. The data presented in figure.6 was fitted to the Langmuir equation [27] in linearized form [13]:

$$\frac{C_e}{q_e} = \frac{1}{q_m K_L} + \frac{1}{q_m} C_e \quad (5)$$

where C_e (mg/L) represents as the equilibrium Cu(II) concentration in solution, q_m (mg/g) denotes as the mono-layer adsorption capacity of Langmuir, and K_L (L/mg) is the over-all adsorption capacity of Langmuir. Plotting C_e/q_e over C_e yields a straight line with the intercept, $1/(q_m K_L)$ and the slope, $1/q_m$ to determine the parameters value. The Langmuir plot is shown in figure 7. The Freundlich equation [28] is linearized [13] and presented as:

$$\log q_e = \frac{1}{n} \log C_e + \log K_F \quad (6)$$

where K_F (L/mg) represents the over-all adsorption capacity of Freundlich, $1/n$ is the Freundlich adsorption intensity. By plotting $\log q_e$ over $\log C_e$ yields a straight line with the slope, $1/n$ and the intercept, $\log K_F$ to determine the parameters value. The Freundlich plot is shown in figure 8.

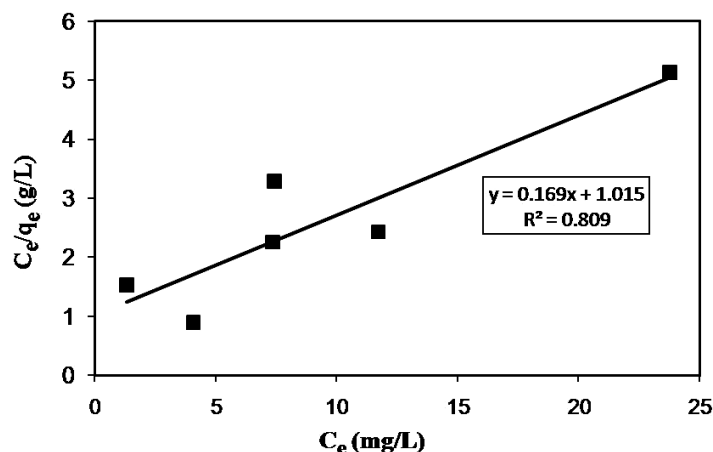


Figure 7. Langmuir isotherm for Cu(II) adsorption by the OPEFB AC. Experimental condition: 100 mL aqueous solution of Cu(II) ions with initial concentration varied from 10 to 70 mg/L, 1 g the OPEFB AC, 75 rpm magnetic stirring, room temperature of 300.15 K (± 2 K), neutral pH and 1 atm with sampling time of 150-min.

As can be seen in figures 7 and 8, the R^2 value on the Cu(II) adsorption isotherm for the Langmuir and Freundlich equations is approximately 0.809 and 0.629, respectively. The mono-layer adsorption capacity and the over-all adsorption capacity of Langmuir obtained was 5.917 mg/g and 0.166 L/g, respectively. Meanwhile, the parameters in the Freundlich model were calculated, and the over-all adsorption capacity and adsorption intensity of Freundlich obtained was 1.006 L/mg and 1.852 respectively. Overall, the Cu(II) adsorption isotherm by the OPEFB AC follows the Langmuir equation, it is favourable adsorption of Cu(II) ions on the OPEFB AC, and each active site of the OPEFB AC adsorb only one molecule of Cu(II) ion to form a monolayer on the OPEFB AC surface.

As highlighted in figures 7 and 8, the correlation coefficients (R^2) of the Cu(II) adsorption isotherm linear plot is approximately 0.95 and 0.57 for the Langmuir and Freundlich models respectively. The parameters based on the Langmuir equation were obtained, and the q_m and K_L values were 5.92 mg/g and 0.17 L/mg, respectively. Meanwhile, the parameters based on the Freundlich equation were calculated, and the K_F and n values were worked out to be 1.01 L/mg and 1.85, respectively. Overall, the adsorption isotherm of Cu(II) on the OPEFB activated carbon follows the Langmuir model. The Cu(II) adsorption capacity by the OPEFB AC is less than the ones by green tea (6.37 mg/g), coarse tea (7.36 mg/g), Cassava peel (11.35 mg/g) and Brazil nut shells (19.45 mg/g) [10], [11]. Therefore, further studies might be needed to investigate a new method of utilisation activated carbon from the OPEFB to get higher Cu(II) adsorption capacity.

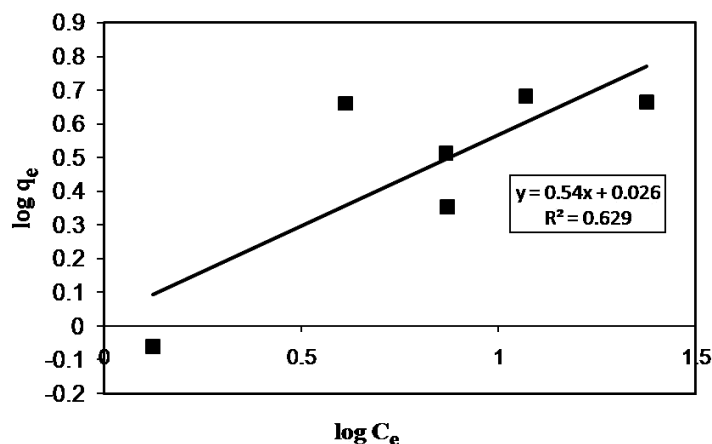


Figure 8. Freundlich isotherm for Cu(II) adsorption by the OPEFB AC. Experimental condition: 100 mL aqueous solution of Cu(II) ions with initial concentration varied from 10 to 70 mg/L, 1 g the OPEFB AC, 75 rpm magnetic stirring, room temperature of 300.15 K (± 2 K), neutral pH and 1 atm with sampling time of 150-min.

4. Conclusions

Oil palm empty fruit bunch (OPEFB) was used to prepare activated carbon by physical activation (pyrolysis at 873.15 K in a furnace for 1 h) and chemical activation (0.01 M HCl for 2 h). Based on the FTIR analysis, it was found that the chemical functional groups such as phenol, alcohol, aldehyde, alkene, ether, ester were removed during the activation leading to the the formation of pores on the OPEFB AC, as also shown by the SEM analysis. The FTIR and SEM analyses was also in line with the results of BET analysis. Experiments in batch mode consisting of 1 g the OPEFB AC in 100 mL Cu(II) aqueous solution with the initial concentration in the range of 10-70 mg/L, magnetic stirring at 75 rpm, room temperature of 300.15 K (± 2 K), at 1 atm and neutral pH over the contact time in the range of 0-150 min were performed to investigate the effect of contact time and initial Cu(II) concentration in solution on Cu(II) adsorption capacity by the OPEFB AC. As the result, Cu(II) adsorption capacity over contact time and initial concentration was typically exponential trends.

The result of adsorption kinetics study with 58.71 mg/L initial Cu(II) concentration showed that Cu(II) adsorption onto the OPEFB AC followed the pseudo-second-order kinetics with the correlation coefficients (R^2), kinetics rate constant and equilibrium adsorption capacity being 0.99, 4.831 mg/g and 0.21/min, respectively for. Moreover, Langmuir equation was reliable to present Cu(II) adsorption onto the OPEFB AC with the R^2 value being 0.99, and the mono-layer and over-all adsorption capacity was determined to 5.92 mg/g and 0.17 L/mg, respectively. Further studies might be needed to investigate a new utilisation method to produce the OPEFB AC with higher Cu(II) adsorption capacity.

References

- [1] Hawkes S J 1997 *J. Chem. Educ.* **74** 11 1374–80
- [2] Srivastava N K and Majumder B C 2008 *J. Hazard. Mat.* **151** 1 1–8
- [3] Bala M, Shehu R A and Lawal M 2008 *Bayero J. Pure Appl. Sci.*, **1** 1 6–38
- [4] Yan-Biao G, Hong F, Chong C, Chong-Jian J, Fan X and Ying L 2013 *Pol. J. Environ. Stud.* **22** 5 1357–62
- [5] Dimple L 2014 *Int. J. Environ. Res. Dev.* **4** 1 41–8
- [6] Minamisawa M, Minamisawa H, Yoshioda S and Taki N 2004 *J. Agri. Food Chem.* **52** 18

5606–15

- [7] Theophanides T and Anastassopoulou J 2002 *Crit. Rev. Oncol. Hematol.* **42** 1 57–64
- [8] Eccles H 1999 *Trends Biotechnol.* **17** 12 462–5
- [9] Leung W C, Wong M F, Chua H, Lo W and Leung C K 2000 *Water Sci. Technol.* **41** 12 233–40
- [10] Basso M C, Cerrell E G and Cukierman A L 2002 *Ind. Eng. Chem. Res.* **41** 15 3580–85.
- [11] Moreno P, Carlos J and Giraldo L 2010 *J. Anal. Appl. Pyrol.* **87** 2 188–93
- [12] Baquero M C, Giraldo L, Moreno J C, Suárez-García F, Martínez-Alonso A and Tascón J M D 2003 *J. Anal. Appl. Pyrol.* **70** 2 779–84
- [13] Muslim A, Zulfian, Ismayanda M H, Devrina E and Fahmi H 2015. *J. Eng. Sci. Technol.* **10** 12 1654–66
- [14] Hidayu A R, Mohamad N F, Matali S and Sharifah A S A K 2013. *Procedia Eng.* **68**, 379–84
- [15] Teoh C H 2000 *Land Use and the Oil Palm Industry in Malaysia*. A bridged report produced for the WWF forest information system database under project MY 0057 – Policy assessment of Malaysia conservation issues, Kinabatangan, November 2000
- [16] World Growth 2009 *World Growth Palm Oil Green Development Campaign: Palm Oil — The Sustainable Oil*. A Report by World Growth September 2009. Available online at http://www.worldgrowth.org/assets/files/Palm_Oil.pdf, (accessed 7 December 2015)
- [17] ResearchInChina 2015 China activated carbon industry report, 2014–2017
- [18] Muslim A in press Australian pine cones-based activated carbon for adsorption of copper in aqueous solution *J. Eng. Sci. Technol.*
- [19] Yang T and Lua A 2003 *J. Colloid Interface Sci.* **267** 2 408–17
- [20] Silverstein R M, Bassler G C and Morrill T C 1981 *Spectrometric Identification of Organic Compounds* 4th ed. (New York: Wiley–Interscience)
- [21] Hesas R H, Niya A A, Daud, W M A W and Sahu J N 2003 *Bio Resources* **8** 2 2950–66
- [22] Wong K K, Lee C K, Low K S and Haron M J 2003 *Chemosphere* **50** 23–8
- [23] Mengistie A A, Siva R T, Prasada R A V and Singanan M 2008 *Bull. Chem. Soc. Ethiop.* **22** 3 349–60
- [24] Tseng R L and Tseng S K 2005 *J. Colloid Interface Sci.* **287** 2 428–37
- [25] Lagergren S 1989 *K. Sven. Vetensk. Akad. Handl.* **24** 4 1–39
- [26] Ho Y S, Wase D A J and Forster C F 1996 *Environ. Technol.* **17** 71–7
- [27] Langmuir I 1918 *J. Am. Chem. Soc.* **40** 9 1361–1403
- [28] Freundlich H 1906. *J. Phys. Chem.* **57** 384–410